Effect of horizontal grid resolution on simulations of oceanic CFC-11 uptake and direct injection of anthropogenic CO_2

M. E. Wickett
Center for Applied Scientific Computing, Lawrence Livermore National Laboratory, Livermore, California, USA

K. Caldeira and P. B. Duffy
Climate and Carbon Cycle Modeling Group, Lawrence Livermore National Laboratory, Livermore, California, USA

Received 6 September 2001; revised 3 June 2002; accepted 24 February 2003; published 14 June 2003.

[1] We simulate direct injection of CO_2 and uptake of CFC-11 in a global, three-dimensional ocean general circulation model using two model resolutions: a coarse resolution of 4° in longitude by 2° in latitude and a finer resolution of 1° in both longitude and latitude. We assess the impact of resolution on the relative effectiveness of ocean carbon sequestration for four different injection sites: New York at 710 and 3025 m depths and San Francisco at 710 and 3025 m depths. Results show that deep injection is generally effective, with relatively small differences in retention, transport, and fluxes between the two resolutions. Results for the change in ocean pH due to CO_2 injection show that resolution does limit the details at sufficiently small scales, with the finer resolution showing greater maximum pH changes. Model predictions of CFC-11 uptake generally have shallower penetration than is seen in observations, and the differences between the model resolutions are much smaller than the differences between either simulation and the observations. There is no persuasive evidence of improvement of large-scale results with globally higher horizontal resolution in these non-eddy-resolving simulations to justify the computational expense. However, when local details are the primary interest, the use of higher resolution may be justified. We suggest that the best approach to improving the results of coarse-resolution ocean models is not to globally increase horizontal resolution outside of the eddy-resolving regime, but rather to pursue other approaches such as improved numerical methods, better parameterizations of sub-grid-scale processes, better forcing data, or perhaps local resolution increases. *INDEX TERMS:* 1635 Global Change: Oceans (4203); 4255 Oceanography: General: Numerical modeling; 4808 Oceanography: Biological and Chemical: Chemical tracers; 4805 Oceanography: Biological and Chemical: Biogeochemical cycles (1615); 1050 Geochemistry: Marine geochemistry (4835, 4850); *KEYWORDS:* ocean, model, resolution, CO_2, sequestration, CFC

Citation: Wickett, M. E., K. Caldeira, and P. B. Duffy, Effect of horizontal grid resolution on simulations of oceanic CFC-11 uptake and direct injection of anthropogenic CO_2, *J. Geophys. Res.*, *108*(C6), 3189, doi:10.1029/2001JC001130, 2003.

1. Introduction

[2] Because of a characteristic timescale of about 1000 years for vertical overturning in the ocean, simulations of the ocean circulation require thousands of simulated years to approach equilibrium (i.e., for the solution to adjust to stationary boundary conditions). Because of limited computer resources, multimillennial simulations using global eddy-resolving ocean models are not possible at present, and are not anticipated in the near future. Thus, for simulations of climate change and of the ocean carbon cycle, there is a continuing need for coarse (non-eddy-resolving) global ocean model simulations. Despite this, it is unclear to what extent globally higher resolution improves the results of ocean models outside the eddy-resolving regime.

[3] We have performed simulations of the global ocean in which the model has been integrated to near equilibrium with its boundary conditions. To our knowledge, the one degree resolution simulations presented here are the highest resolution simulations of this kind performed to date. *Duffy et al.* [2002] assessed the degree to which model resolution affects the equilibrium solution of circulation, temperature, and salinity. Here we assess the effects of horizontal model resolution on time-dependent predictions of CO_2 injection and CFC-11 uptake. Since the equilibrium behavior of the model affects the time-dependent results given here, we also present a summary of the equilibrium results at the beginning of the results section.

[4] Direct injection of CO_2 into the ocean interior has been proposed as a means of slowing the accumulation of carbon dioxide in the atmosphere, thereby mitigating global climate change [*Marchetti*, 1977]. Fossil fuel CO_2 uptake by the oceans is largely limited by mixing processes that govern the relatively slow transfer of excess atmospheric

CO_2 to the deep ocean [*Sarmiento et al.*, 1992; *Caldeira and Duffy*, 2000]. The idea of direct CO_2 injection is to place fossil fuel carbon dioxide directly into the middepth waters, bypassing the slow natural transport of anthropogenic carbon [*Herzog et al.*, 2001]. Two areas of ongoing research are (1) prediction of how long carbon will be retained in the ocean as a function of the location and depth of injection [e.g., *Orr et al.*, 2001], and (2) prediction of the distribution of CO_2 and pH changes resulting from direct injection and the biotic consequences of those changes.

[5] Simulations of the uptake of atmospheric chlorofluorocarbons (CFCs) have proven useful for validating ocean models and testing their sensitivities to changes in model configuration [e.g., *England*, 1995; *Robitaille and Weaver*, 1995; *Caldeira and Duffy*, 1998]. The usefulness of CFCs as diagnostic tracers is attributable to a lack of natural sources combined with availability of measurements of ocean concentrations. We simulate the historical oceanic uptake of CFC-11 due to industrial release and evaluate the sensitivity to model resolution. In contrast to the CO_2 simulations, in which the tracer source is localized and interior to the ocean, the source of CFC-11 is atmospheric and global, providing a different character for transient tracer response to horizontal model resolution.

2. Model Description

[6] The simulations presented here were performed with the Lawrence Livermore National Laboratory (LLNL) ocean/sea ice model, a primitive equation, finite difference, level coordinate model based on the Modular Ocean Model (MOM) of the Geophysical Fluid Dynamics Laboratory. Enhancements include the addition of the Gent-McWilliams eddy parameterization [*Gent and McWilliams*, 1990], coupling to a parallel version of the Oberhuber sea ice model [*Oberhuber*, 1993], and replacement of the "rigid lid" approximation with an explicit free surface approach [*Killworth et al.*, 1991]. The LLNL model is described in more detail by *Duffy and Caldeira* [1997] and by *Wickett et al.* [2000].

[7] Two grid resolutions are used, both with a global domain: a case with 1° resolution is referred to as the "fine" case, while a case with 4° longitudinal by 2° latitudinal resolution is referred to as the "coarse" case. Because of the explicit finite difference numerics used, the fine case has a 32-fold increase in computational cost relative to the coarse case (a factor of 8 from the increase in cell count, and a factor of 4 from the decrease in stable time step size.)

[8] Topography (see Figure 1) is essentially realistic, but has been lightly smoothed to assure that topographic changes generally occur on a larger scale than the model grid, minimizing numerical problems. Both horizontal resolutions use the same 23 levels in the vertical. All surface forcings are obtained by linear interpolation in time between monthly mean climatological data. Wind forcing (i.e., surface momentum flux) is from *Hellerman and Rosenstein* [1983]. Surface salinities over open ocean are restored to *Levitus and Boyer* [1994] data with a time constant of 58 days. Under sea ice, fluxes of fresh water are calculated from the formation and melting of sea ice, with no restoring used. Sensible, latent, long-wave, and short-wave components are calculated independently using climatological atmospheric data and bulk parameterizations [*Oberhuber*, 1993].

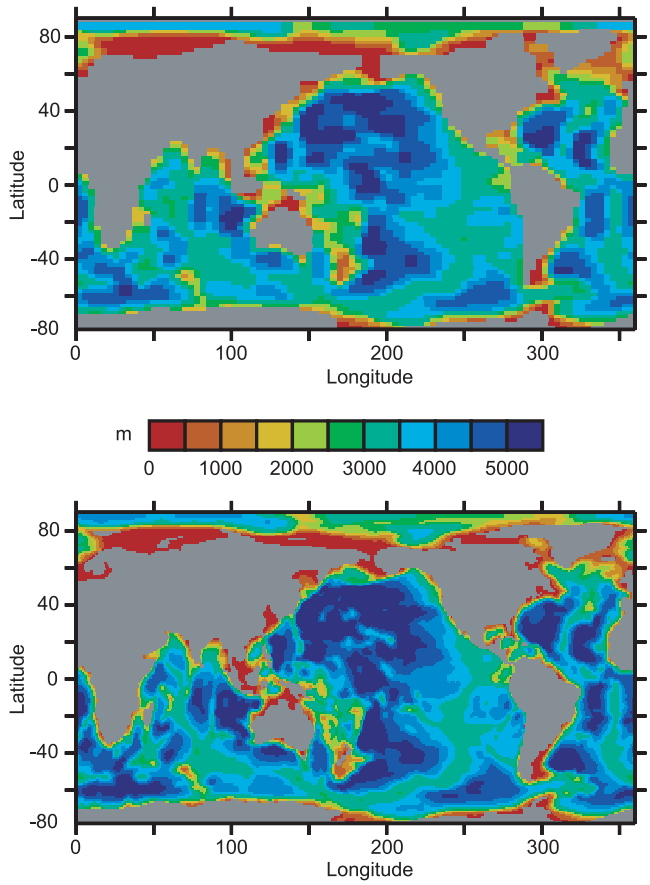

Figure 1. The topography used in (top) the coarse case and (bottom) the fine case. Both use the same 23 levels in the vertical.

[9] Exactly how mixing coefficients should vary with grid resolution is not widely agreed upon. As argued by *McWilliams* [1996, 1998] and further described by *Duffy et al.* [2002], we use the same tracer mixing coefficients for both (non-eddy-resolving) grid resolutions. The isopycnal tracer mixing coefficient is set to 2×10^7 cm^2/s with a thickness diffusion of 10^7 cm^2/s. The vertical tracer mixing coefficient varies from 0.2 cm^2/s at the surface to 10.0 cm^2/s at depth. Since model momentum mixing (viscous) coefficients are larger than physically justifiable, we use the smallest value for each grid resolution which produces a solution that is stable and relatively free of numerically induced noise. Also, to minimize the occurrence of vertical Peclet-type instabilities [*Weaver and Sarachik*, 1991], the horizontal viscosity, A_H, is given latitudinal dependence according to, $A_H = A_0 \times [1 + 6e^{-(\phi/30)^2}]$, where A_0 is a scalar and ϕ is latitude in degrees. For the coarse case, $A_0 = 10^9$ cm^2/s, and for the fine case, $A_0 = 10^8$ cm^2/s. The vertical viscosity coefficient is set to 20 cm^2/s for both cases.

[10] Both carbon and CFC-11 are assumed to be conservative tracers in the ocean interior for the simulations presented here. Global ocean carbon inventories are affected by air-sea fluxes and directly injected carbon, and global ocean CFC-11 inventories are affected only by air-sea

fluxes. The representation of the carbon cycle and of CFC-11, including gas exchange and chemistry, are as defined by the "Abiotic" and "CFC" configurations of the second phase of the Ocean Carbon-cycle Model Intercomparison Project, or OCMIP-2 (http://www.ipsl.jussieu.fr/OCMIP). Following these protocols, air-sea fluxes of CO_2 and CFC-11 are calculated using the classical formulation, $F = k(\alpha[A]_{atm}\frac{P}{P_0} - [A]_{surf})$ where α is the tracer solubility from *Warner and Weiss* [1985], calculated from model sea surface temperature and salinity; $[A]_{atm}$ is the atmospheric partial pressure of the tracer; P is the monthly total air pressure at sea level from *Esbensen and Kushnir* [1981]; P_0 is 1 atm; $[A]_{surf}$ is the model sea surface tracer concentration; and k is the air-sea gas transfer velocity from *Wanninkhof* [1992] given by, $k = k_0 (1 - R) (u^2 + \langle v \rangle) (Sc/660)^{-1/2}$, where R is the sea ice fraction, prescribed by the *Walsh* [1978] and *Zwally et al.* [1983] climatologies; Sc is the Schmidt number of the gas, calculated from model sea surface temperature with the formulation of *Zheng et al.* [1998]; u and $\langle v \rangle$ are the monthly mean and variance of instantaneous wind speed at 10 m, respectively, as described by *Boutin and Etcheto* [1997] and *Orr* [2001]; and k_0 is a constant that has been calibrated so that the global mean k for CO_2 matches the *Broecker et al.* [1986] radiocarbon-calibrated estimate of 0.061 mol C/(m^2 yr μatm). The direct injection simulations were performed under a nominal preindustrial atmosphere with 278 ppm CO_2. Atmospheric CFC-11 concentrations are assumed uniform for each hemisphere poleward of 10° latitude and vary linearly in between, with the time history given by *Walker et al.* [2000].

[11] As specified by the OCMIP-2 protocol, we integrated the coarse case until the globally integrated air-sea CO_2 flux was less than 0.01 PgC/yr. This corresponded to over 4000 surface tracer years, and more than 30,000 years in the deepest model layers using the time step splitting and deep ocean acceleration techniques described by *Bryan* [1984] and *Danabasoglu et al.* [1996], respectively. Then an additional 20 years of integration were performed without deep ocean acceleration. The fine case was initialized from the results of the coarse case integration, regridded to the higher resolution. Then it was integrated for over 2500 surface tracer years plus 20 years without deep ocean acceleration to bring it to an equilibrium solution prior to beginning the time-dependent simulations.

[12] For each of the two model resolutions, we performed simulations of CO_2 injection near New York and near San Francisco, at depths of 710 m and 3025 m. All simulated CO_2 injections were at the rate of 0.1 PgC/yr, sustained for 100 years. The CO_2 was assumed to instantaneously dissolve in a single grid cell at the injection location. Simulations of CFC-11 uptake from the atmosphere were performed for a simulated time period from 1930 through 1999.

3. Results and Discussion

3.1. Equilibrium Results

[13] *Duffy et al.* [2002] compared the equilibrium results of one fine simulation and three coarse simulations. The fine simulation and one of the coarse simulations used the same configuration as presented here, while the additional two coarse simulations had lowered viscosity and no high-latitude filtering, respectively. In general the fine results were closer to observations than the coarse results, although only slightly so. In particular, the following aspects of the fine simulation were more realistic: temperatures and salinities in the Arctic Ocean, temperatures in the deep Southern Ocean, and vertical temperature gradients in the thermocline. Differences attributable to sensitivity to changing viscosity included meridional overturning and the strength of flows in the Antarctic Circumpolar Current. Results which were relatively unchanged included the extent and thickness of sea ice and the latitudinal heat transfer. The differences between the fine and coarse results were always much smaller than the differences between any simulation and available observations. In addition, the differences between the high- and low-viscosity coarse cases were larger than the differences between the low-viscosity coarse and fine cases. Thus our results show that the near-equilibrium mean solution of our model is quite insensitive to resolution for simulations outside the eddy-resolving regime.

3.2. Direct Injection

[14] As described above, we performed simulations of CO_2 injection near New York and near San Francisco, at depths of 710 m (referred to as "shallow") and 3025 m ("deep"). All simulated CO_2 injections were at the rate of 0.1 PgC/yr, sustained for 100 years.

3.2.1. Retention and Fluxes

[15] The percentages of injected CO_2 remaining in the ocean globally at the end of the 100 years of injection are shown in Table 1. Since the atmospheric CO_2 concentration is held fixed for these simulations, all of the CO_2 injected would eventually escape from the ocean if the injection were stopped. For the two deep injection locations, nearly all of the injected CO_2 remains in the ocean after 100 years, and there is very little difference in overall retention between the results of the coarse and fine cases. For the shallow injections, there is as much as 5% difference between the coarse and the fine, with the two locations producing differences of opposite sign.

[16] The column inventories (i.e., vertically integrated concentrations) of injected CO_2 at the end of 100 years of continuous injection (Figure 2) and the inventories by basin (Table 1 and Figure 3) show the spatial distribution of the injected carbon. Both of the San Francisco injections show very similar distributions for the two resolutions. There is a slightly higher column inventory in the equatorial Atlantic for the deep fine case than for the coarse. The shallow New York injection produces very similar distributions for the two resolutions given the difference in global retention.

[17] The deep New York injection shows much larger differences between the two resolutions. In the coarse case, there is considerably more transport southward and much less transport northward than in the fine case, resulting in very different Atlantic ocean distribution and Northern ocean inventory. The Southern, Indian, and Pacific ocean inventories are similar, however, such that 97.5% and 97.9% of the injected carbon remains in the Atlantic and Northern oceans for the coarse and fine cases, respectively.

[18] To quantify the differences in the spatial distributions, we performed statistical comparisons of the coarse and fine

Table 1. Percentages of Injected CO_2 Remaining in the Ocean After 100 Years for Each Injection Location, Injection Depth, and Grid Resolution, Broken Down by Basin

	710 m		3025 m	
Region	Coarse	Fine	Coarse	Fine
	N.Y.			
Global Total	72.9	77.0	99.51	99.66
Atlantic Ocean	64.2	67.2	96.9	93.9
Northern	50.8	53.5	59.4	66.9
Equatorial	11.4	11.7	29.6	20.8
Southern	2.0	2.1	7.9	6.2
Pacific Ocean	0.0	0.0	0.0	0.0
Indian Ocean	0.2	0.2	0.9	0.6
Northern Ocean	8.2	9.1	0.6	4.0
Southern Ocean	0.2	0.4	1.0	1.1
	S.F.			
Global Total	90.2	88.8	99.97	99.98
Atlantic Ocean	0.0	0.0	0.0	0.0
Pacific Ocean	88.5	87.4	99.86	99.86
Northern	64.5	63.5	73.8	71.8
Equatorial	22.4	22.1	24.1	25.9
Southern	1.6	1.7	2.0	2.2
Indian Ocean	1.4	1.0	0.0	0.0
Northern Ocean	0.2	0.3	0.0	0.0
Southern Ocean	0.1	0.1	0.1	0.1

results for both the column inventory and zonal mean, the results of which are shown in Table 2. In making these calculations, the fine results were first regridded to the coarse resolution by area weighted averaging. We excluded cells which were not completely water at both grid resolutions. Thus cells for which direct comparison cannot be made because of differences in ocean volume are not included. The error is calculated as the mean absolute difference between the fine and coarse solutions normalized by the mean of the fine solution. We also computed an area-weighted least squares linear regression predicting the regridded fine results from the coarse results. Thus the R^2 column shows the fraction of spatial variance in the regridded fine case results that can be explained as a linear mapping from the coarse results.

[19] Both measures are sensitive to spatial shifts of the results, such that identical solutions shifted by one grid cell could produce large error and low correlation. In addition, the error measure is sensitive to scaling of the results, such that solutions with identical spatial distribution but magnitudes related by a multiplicative scalar could produce large error but would still have high correlation.

[20] The primary difference in Table 2 is between the fine and coarse case of the deep New York injection, as described above. *Duffy et al.* [2002] discussed the flows in the runs and found that changing viscosity had a very large effect on strength of flows. In fact, when looking at the Antarctic Circumpolar Current, there was a large increase in the flow strength in the fine case over the coarse. However, this difference was nearly eliminated in a coarse run using the same lowered viscosity coefficient as the fine case. The differences in the deep New York injection results appear to be caused by the difference in the flow field near the location of the injection. Though we did not perform a coarse injection simulation with the lower viscosity, the flow field for the lower-viscosity coarse case is indeed more similar to the fine case than to the standard viscosity coarse case.

[21] Further spatial differences are shown in the fluxes of injected CO_2 at the end of the 100 years (Figure 4). Negative values indicate fluxes to the atmosphere. The fluxes for both of the New York injections are very similar. The difference in north/south transport seen in the column inventories of the deep injection is manifested only as a small increase in equatorial flux and a slight decrease in longitudinal extent of Arctic fluxes for the fine case.

[22] The largest flux differences appear in the shallow San Francisco injection. Though this case showed little difference in the column inventories, there is a decrease in equatorial Pacific fluxes and an increase in northwestern Pacific fluxes in the fine case relative to the coarse. There are increased fluxes in the equatorial Atlantic as well, corresponding to the increased column inventory there. The deep San Francisco injection also shows a slight decrease in northwestern Pacific fluxes in the fine case relative to the coarse.

3.2.2. The pH Changes

[23] It has been recognized that the greatest impact from deep-sea CO_2 injection is likely to be a result of the change in deep-sea pH [*Magnesen and Wohl*, 1993]. It is important to note that the ocean is naturally sequestering anthropogenic carbon dioxide. As the fossil fuel reserves are burned, even with no injection sequestration of CO_2, deep-sea pH is expected to decrease by as much as 0.5 pH units [*Herzog et al.*, 1995]. *Magnesen and Wohl* [1993] estimate that changes in ocean pH of more than 0.2 units will have some detectable biological impact.

[24] Here we present the change in pH due to each of the injection sources. Ocean pH changes were estimated using the carbonate chemistry calculation described by *Takahashi et al.* [1982] and *Peng et al.* [1987]. Figure 5 shows volume of ocean versus change in pH for each of the four injection locations and for each grid resolution. That is, for a given change in pH, the volume of the ocean which has a change at least that large is displayed. The total ocean volumes for the coarse and fine grids are 1.34×10^{18} m^3 and 1.40×10^{18} m^3, respectively.

[25] We note that for each case and location, the largest pH change has a volume which is equal to the volume of the single grid cell at the injection location. This is expected as long as the grid cell size is large compared to the characteristic size of the injection site. Thus resolution is obviously limiting the maximum predicted pH change and its associated volume. Maximum predicted pH changes are greater for the fine case because the injected CO_2 is being added initially to a smaller volume. To accurately predict pH changes near the point of injection, a very high resolution limited domain model would probably be the appropriate tool.

[26] The volume scale in Figure 5 only encompasses about 1% of the ocean volume. For lower pH changes the fine and coarse results agree well in predicted volume. Thus for more than 99% of the ocean volume the results are very similar. Since there are on the order of 10^6 grid cells in the coarse case, the results tend to agree when the perturbation involves more than 100 or so coarse cells. This suggests a scale on which a coarse GCM is the appropriate tool for viewing pH change or other necessarily resolution-dependent quantities.

[27] These injection results also suggest that while the overall effectiveness of CO_2 injection can be calculated with coarse horizontal resolution, detailed results may require higher resolution for accuracy. For example, to calculate the location of the largest fluxes, the detailed areas of highest

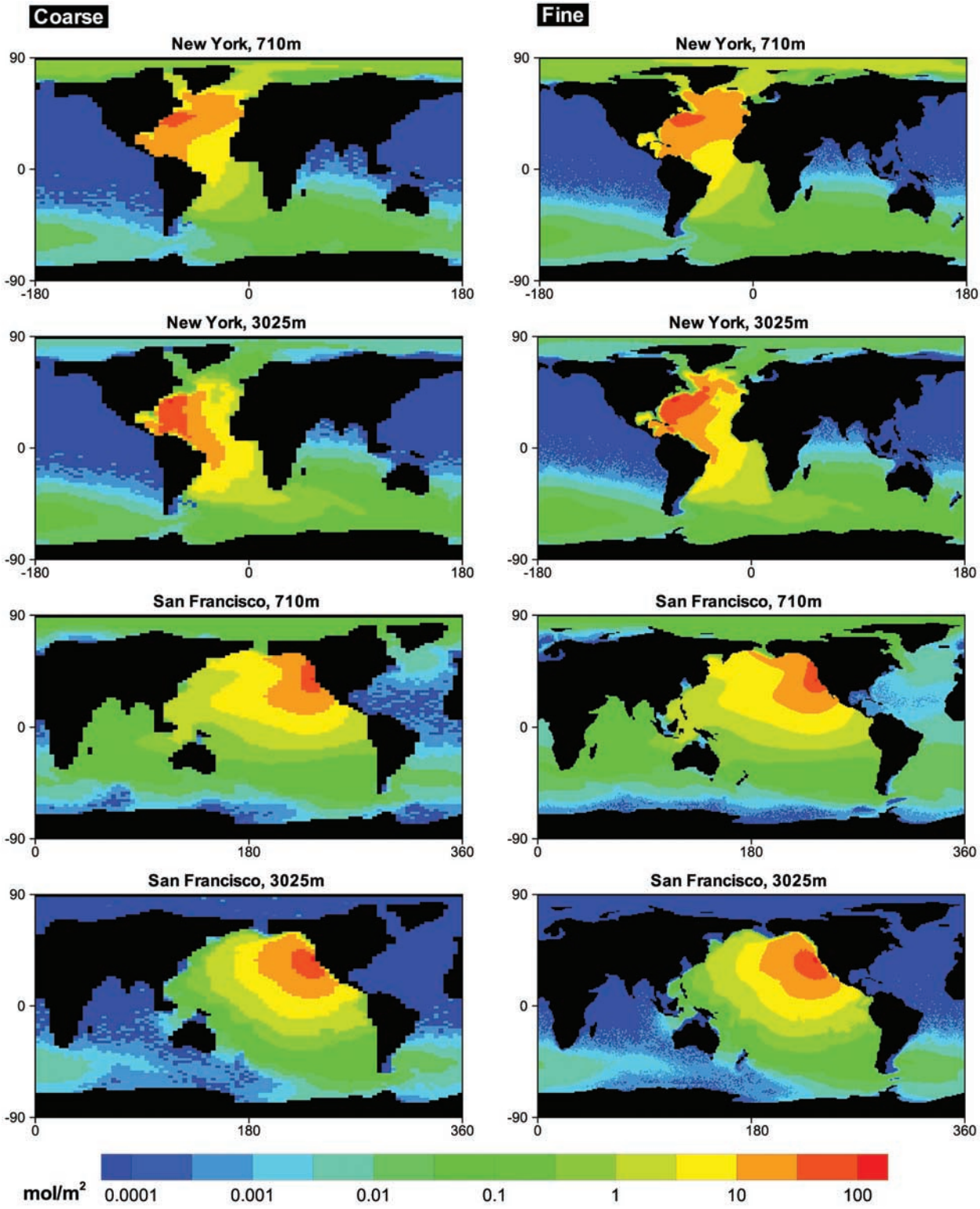

Figure 2. Column inventories (i.e., vertically integrated concentrations) of injected CO_2 after 100 years. The solutions for the two resolutions are very similar for each injection site (note the log scale).

increase in concentration, or the extremes of pH change, an increase in resolution may be necessary.

3.3. CFC-11

[28] The direct injection simulations test the behavior of the model transport for tracers released in the ocean interior. To test the behavior of the transport for tracers absorbed from the atmosphere through the ocean's surface, we performed simulations of oceanic uptake of atmospheric CFC-11.

[29] *Dutay et al.* [2002] compared CFC-11 results from 13 global ocean models, including the LLNL model. The

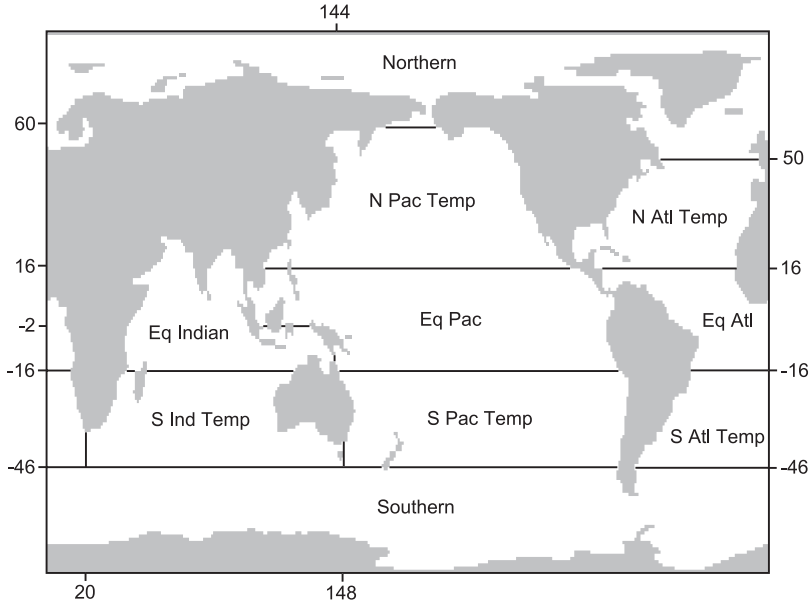

Figure 3. The basins used for the retention and inventory results.

global inventory of CFC-11 was shown to follow the increase of the CFC-11 partial pressure in the atmosphere. This is also true for the simulations presented here, and the results are shown in Figure 6. The average global inventory of the 13 models for the year 1989 was approximately 4.8×10^8 moles, with a standard deviation of about 20% and a range of about ±30% about the mean. Both the coarse and fine global inventories are within one standard deviation of the 13 model mean, and the difference between them is less than 5% of the 13 model mean (see Table 3). Thus, with respect to the difference in CFC-11 uptake between coarse-resolution global ocean models the difference between the coarse and fine cases in our model is small.

[30] The relative error of coarse to fine global inventory is about 5.7%. The lower CFC-11 uptake in the fine case is likely a direct result of the smaller areas of convective activity in the fine case given by *Duffy et al.* [2002], especially in the southern ocean.

[31] Further comparing the CFC-11 results from the two model resolutions, Figure 7 shows the column inventories of CFC-11 for the year 1989. The horizontal distributions are very similar in character, but have relatively large differences in individual regions of high column inventory. For example, near the Drake Passage and in the North Atlantic, the coarse case has a larger amount of CFC-11 than the fine case. Also, in the Arctic near 100E, the fine case has a region of high column inventory which is not present in the coarse case.

Table 2. Scaled Absolute Error and R^2 of a Linear Regression of the Column Inventory and Zonal Mean of Injected CO_2 After 100 Years[a]

		Column		Zonal	
Site	Depth	Error	R^2	Error	R^2
N.Y.	710 m	0.171	0.959	0.148	0.963
N.Y.	3025 m	0.442	0.750	0.412	0.798
S.F.	710 m	0.113	0.992	0.184	0.977
S.F.	3025 m	0.074	0.984	0.142	0.974

[a]Comparison is made between coarse results and regridded fine results.

[32] The regional inventories given in Table 3 show the horizontal distribution at a coarser scale. The fractional basin inventories in the Pacific, Northern, and Southern Oceans are very similar, as are those of the Northern and Equatorial Atlantic Ocean and the Equatorial Indian Ocean. The largest differences are in the Southern Atlantic and the Southern Indian Oceans, reflecting the relatively lower inventory near South America and the relatively higher inventory near Australia in the fine case.

[33] To quantify the differences in the spatial distributions, we performed statistical comparisons of the coarse and fine column inventory and zonal mean results, shown in Table 4. As with the CO_2 results, the fine results were first regridded to the coarse resolution, and we excluded cells which were not completely water at both grid resolutions. We then computed a normalized absolute error and an area-weighted least squares linear regression.

[34] The coarse case explains ~85% of the spatial variance of the column inventory of the fine case.

Table 3. Inventories of CFC-11 for Each Grid Resolution for Year 1989, Broken Down by Basin, as Well as the Percentages of the Total Found in Each Basin

	Coarse		Fine	
Region	Inventories, 10^8 moles	%Total	Inventories, 10^8 moles	%Total
Global Total	4.08		3.86	
Atlantic Ocean	0.764	18.7	0.670	17.4
Northern	0.304	7.5	0.294	7.6
Equatorial	0.090	2.2	0.089	2.3
Southern	0.370	9.1	0.288	7.5
Pacific Ocean	1.25	30.6	1.17	30.3
Northern	0.436	10.7	0.400	10.4
Equatorial	0.244	6.0	0.236	6.1
Southern	0.572	14.0	0.529	13.7
Indian Ocean	0.567	13.9	0.628	16.3
Equatorial	0.115	2.8	0.106	2.7
Southern	0.452	11.1	0.522	13.5
North. Ocean	0.427	10.5	0.392	10.2
South. Ocean	1.07	26.2	1.00	25.9

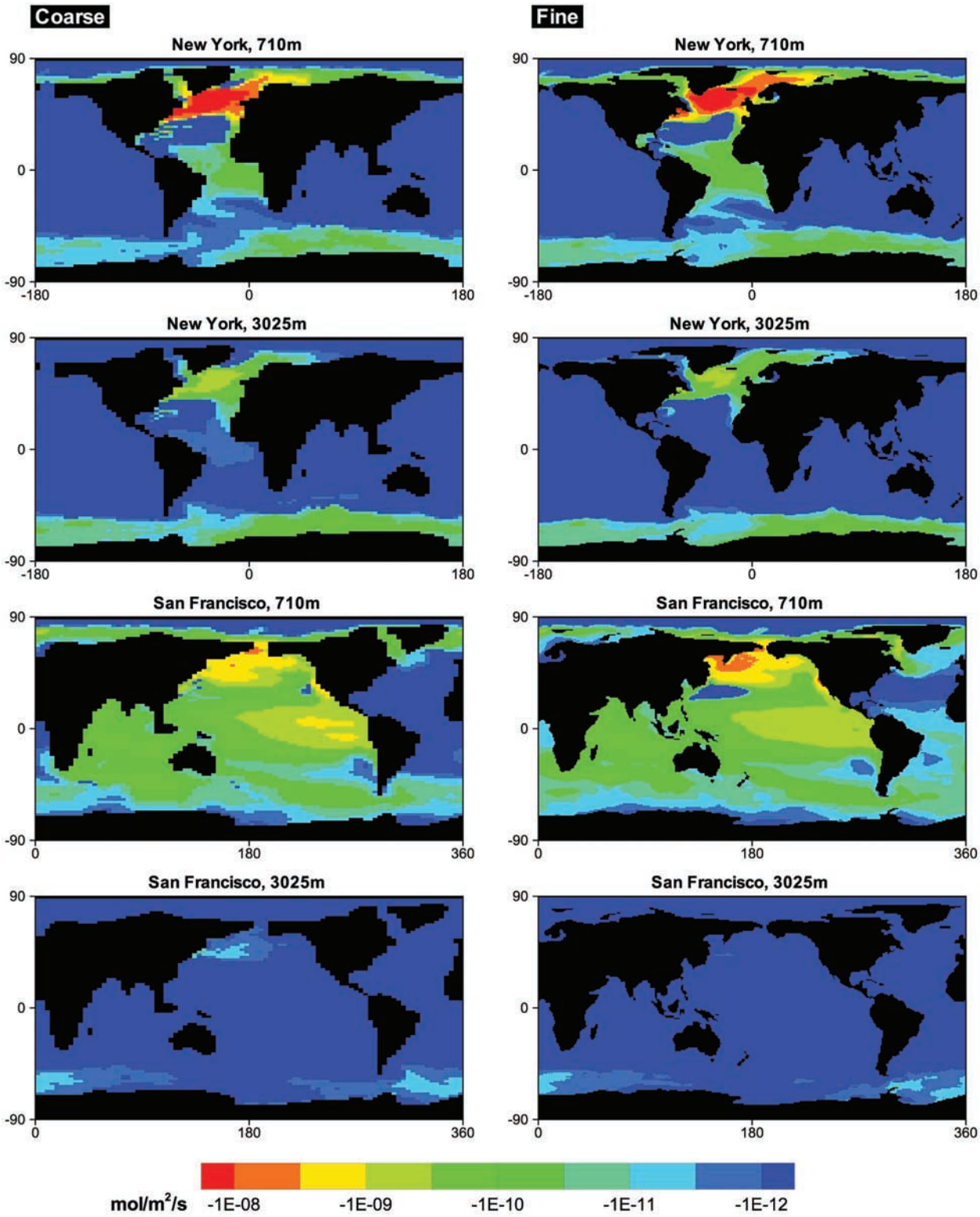

Figure 4. Fluxes of injected carbon after 100 years. Negative values indicate fluxes to the atmosphere. Agreement between the two grid resolutions is very good for all injection locations, with the differences limited to the extreme flux values (note the log scale).

However, the coarse case explains over 99% of the spatial variance in the zonal mean. This occurs primarily because CFC-11 is absorbed from the atmosphere, producing strong vertical gradients at both model resolutions. Furthermore, deepest penetration of CFC-11 in both cases is found in the Southern ocean and in the North Atlantic. The high correlation in the zonal means suggests that the primary difference in the simulations of

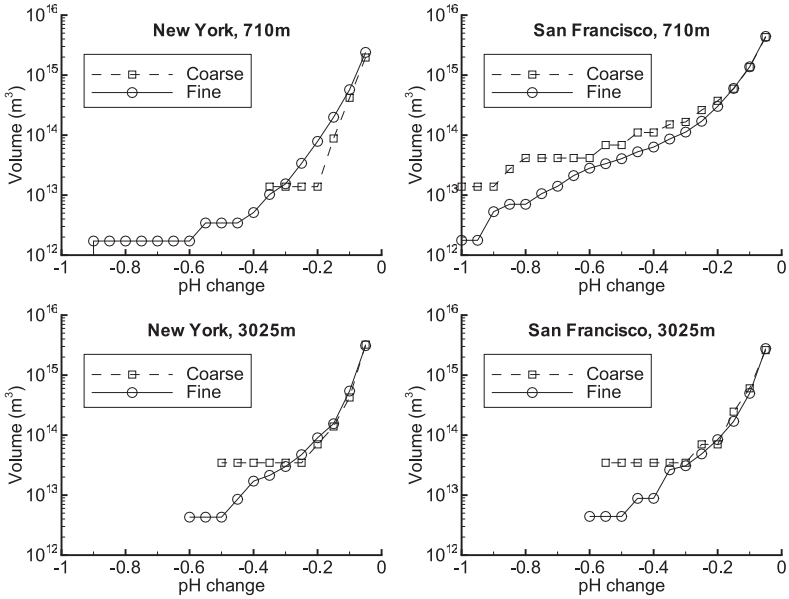

Figure 5. Volume of ocean versus pH change. For a given change in pH, the volume of the ocean which has a change at least that large is displayed. The total coarse-grid volume is 1.34×10^{18} m^3, and the fine-grid volume is 1.40×10^{18} m^3, so the volume scale encompasses about 1% of the ocean volume.

CFC-11 uptake lies in the longitudinal distribution of CFC-11.

[35] The fluxes of CFC-11 for the year 1989 are shown in Figure 8, with positive values indicating downward fluxes. As with the column inventories, agreement between the two grid resolutions is very good. High flux areas in the North Atlantic, North Pacific, Arctic, and the equatorial regions are especially similar for the two cases. While the character of the solution in the southern ocean is also similar for the two cases, the fine case shows more spatial variation.

[36] As previously noted, there was a large increase in the flow strength of the Antarctic Circumpolar Current in the fine case relative to the coarse, attributable to the decrease in viscosity in the former. The change in the details in the southern ocean, both in the fluxes and the column inventory of CFC-11, are likely due to a combination of the change in grid resolution, resolution of bottom topography, and the horizontal viscosity coefficient.

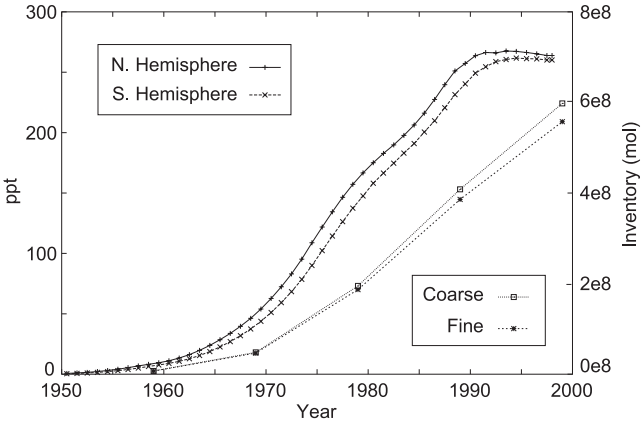

Figure 6. The atmospheric mole fraction in both hemispheres (left axis) and the ocean inventory of CFC-11 (right axis) as a function of time.

[37] Comparison of the two model simulations to three sections of CFC-11 from observations provides a measure of the difference in fidelity between the solutions at the two different resolutions.

[38] Figure 9 shows the AJAX section of the south Atlantic in 1983 [*Warner and Weiss*, 1992]. The fine case has slightly shallower penetration at midlatitudes than the coarse case, with the observations lying somewhere between the two. Both model results display shallower uptake near Antarctica than the observations, with the fine case being slightly closer to the observations in this respect. The fine case results may reflect improved Bottom Water loading of CFC and an improved representation of Circumpolar Deep Water upwelling.

[39] Figure 10 shows the NA20w section of the north Atlantic in 1988 [*Doney and Bullister*, 1992]. Again, shallower uptake is seen in the simulations than in the observations. However, in this section the fine case has shallower penetration throughout compared with the coarse case.

[40] It is likely that the shallower CFC-11 penetration of the Atlantic model results is due in part to the absence of bottom boundary flows in our simulations; these flows bring very cold water (as well as other tracers) into the deep ocean, especially from Antarctic shelf regions. The absence

Table 4. Scaled Absolute Error and R^2 of a Linear Regression of the Column Inventory and Zonal Mean of CFC-11 at Year 1989[a]

Direction	Error	R^2
Column	0.148	0.849
Zonal	0.101	0.991

[a]Comparison is made between coarse results and regridded fine results.

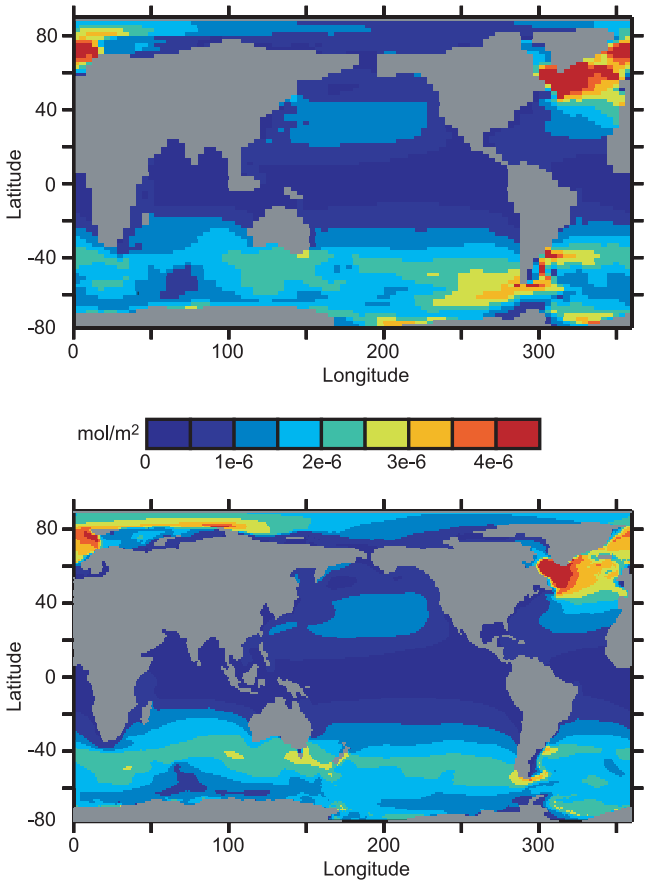

Figure 7. Column inventory of CFC-11 for 1989: (top) the coarse case and (bottom) the fine case.

of these flows in our model has been documented in previous simulations [*Caldeira and Duffy*, 1998] which show that the model does not reproduce elevated concentrations of CFCs observed near the ocean floor. These elevated concentrations are thought to be produced by bottom boundary flows.

[41] Figure 11 shows the WOCE P15S section from the south Pacific, with observations from 1996 [*WOCE Data Products Committee*, 2000] and model results from 1999. In contrast to the Atlantic sections above, there is too much uptake in the model simulations compared with the observations, only a small amount of which is attributable to the 3 year discrepancy in time. Neither model case displays the lower concentration between 2500 and 4000 m seen in the observations, though the fine case is noticeably closer. The depth and extent of the highest concentrations in the simulations agree well overall. For all three sections, the two model simulations are much more similar to each other than either is to the observations.

4. Conclusions

[42] This study examines the effect of horizontal grid resolution on predictions of CO_2 injection and CFC-11 uptake. We compare simulations using a 1° by 1° horizontal mesh to simulations using a 4° (longitude) by 2° (latitude) horizontal mesh. Since none of our simulations resolves mesoscale eddies, our results do not assess the possible importance of resolving eddies in climate simulations. They instead focus on the possible importance of better horizontal resolution of the physics, topography, and forcing within the non-eddy-resolving domain.

[43] The simulated effectiveness of CO_2 injection is not highly sensitive to the global increase in horizontal resolution, but the simulations suggest that detailed results may benefit from a higher resolution, even on relatively coarse scales. Spatial distributions of CO_2 column inventories and fluxes are very similar for the two resolutions at each injection site, with some of the differences attributable to the change in horizontal viscosity. The details of the pH changes near the injection sites are indeed limited by the grid resolution, and the highest changes are not predicted by the coarse case. These near-field issues have little effect on the smaller pH changes in the far field. CFC-11 results also show only small differences between the two simulations, and comparison with observations further emphasizes that those differences are smaller than the differences between either model simulation and the observations.

[44] Our results show that the solution of our model is not highly sensitive to resolution for simulations outside the eddy-resolving regime. There is no persuasive evidence of improvement of large scale CO_2 injection results or CFC-11 uptake with higher resolution in these fairly coarse-resolu-

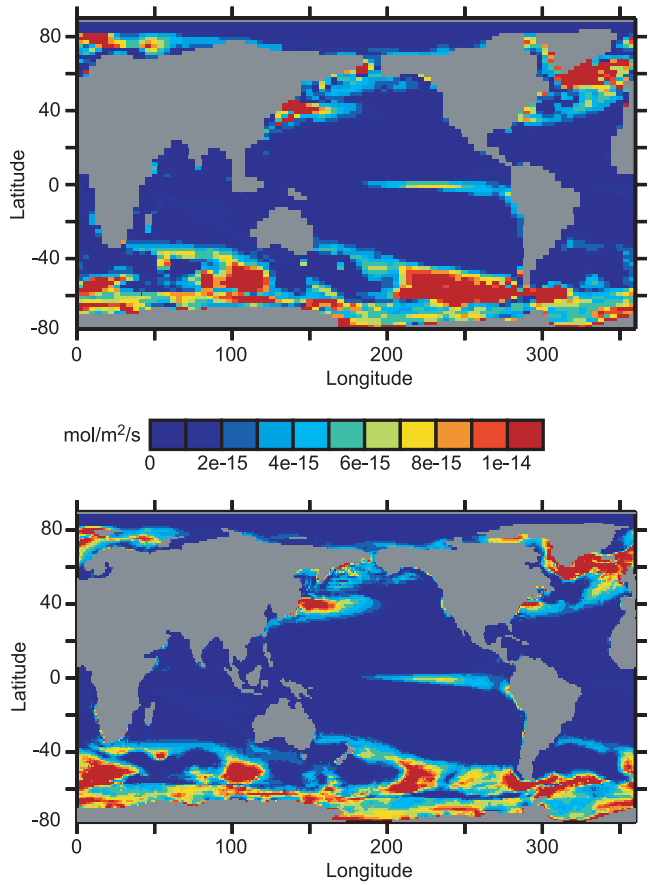

Figure 8. Fluxes of CFC-11 for 1989: (top) the coarse case and (bottom) the fine case.

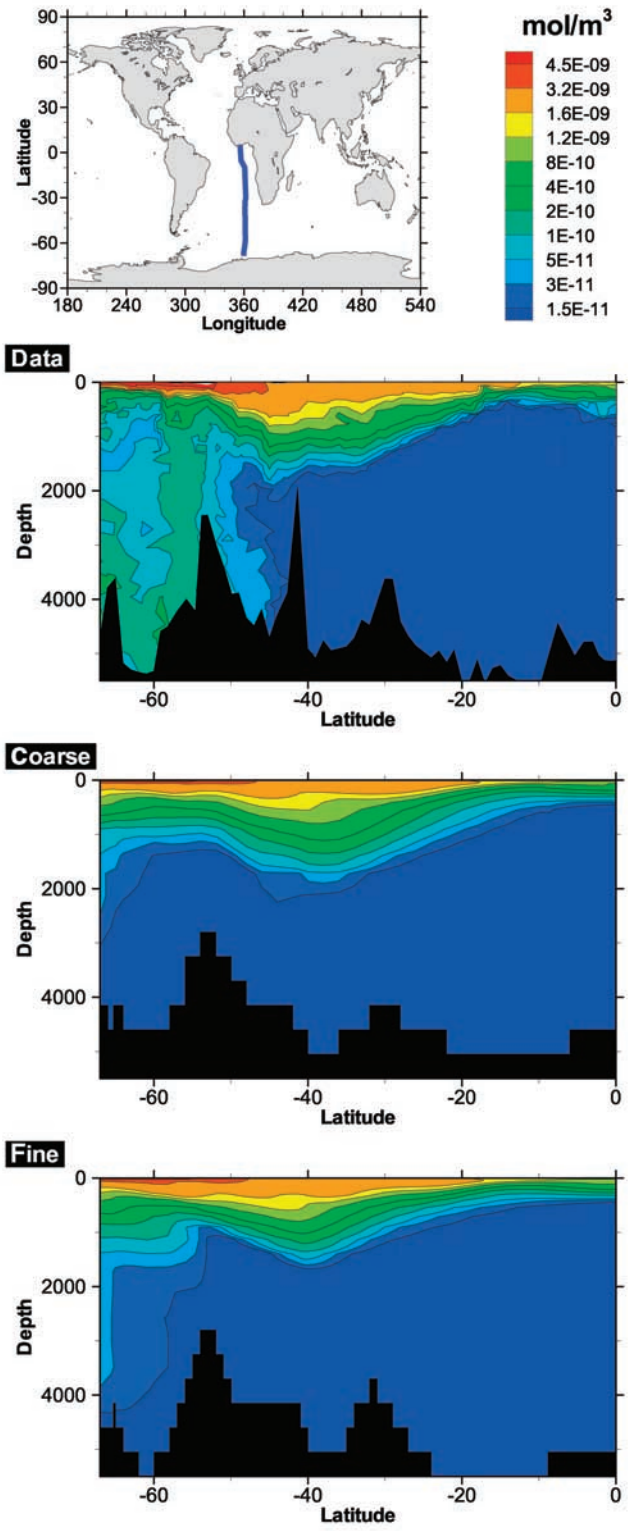

Figure 9. CFC-11 concentration along the AJAX (1983) section [*Warner and Weiss*, 1992].

tion simulations to justify the factor of 32 increase in run time between the simulations presented. However, when local or small-scale details are the primary interest, the use of higher resolution may be justified. Particularly for injection simulations, where small-scale features are of interest in multiple localized areas, mesh refinement may provide improved results without undue computational overhead. We suggest that the best approach to improving the results of coarse-resolution ocean models is not to globally increase horizontal resolution outside of the eddy-resolving regime,

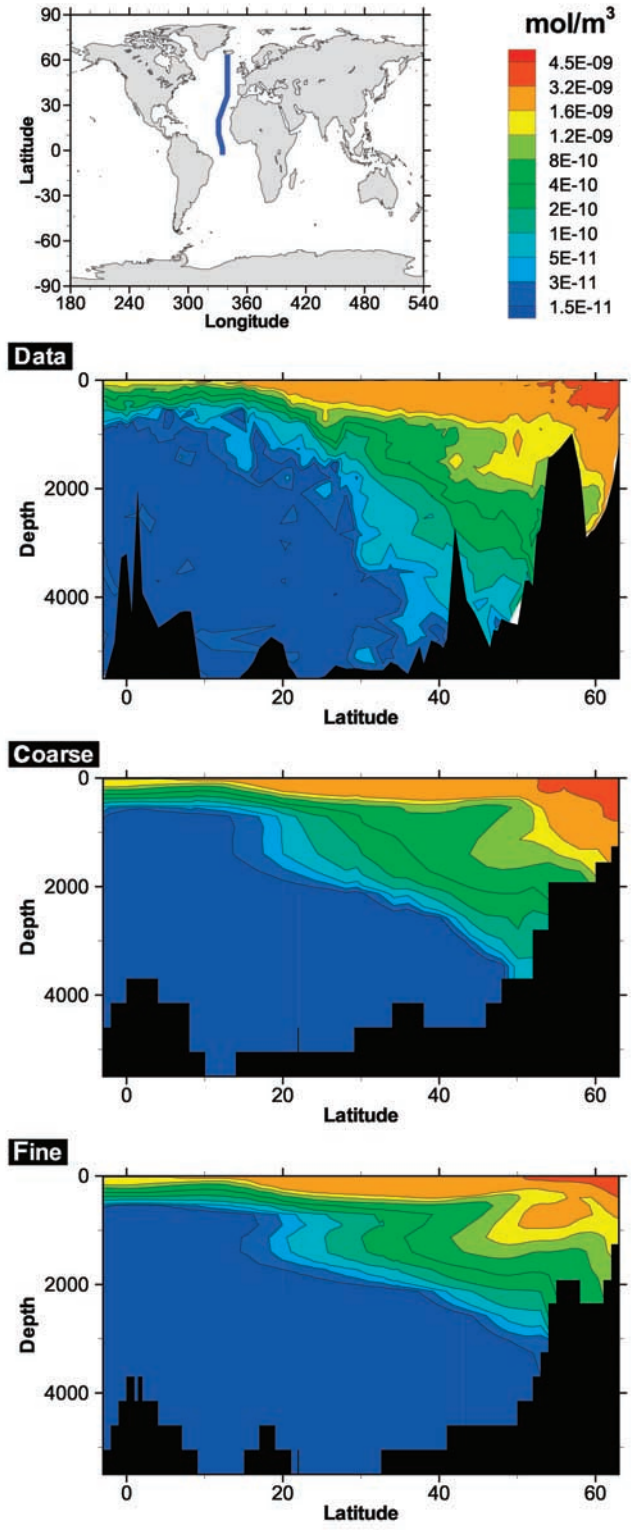

Figure 10. CFC-11 concentration along the NA20W (1988) section [*Doney and Bullister*, 1992].

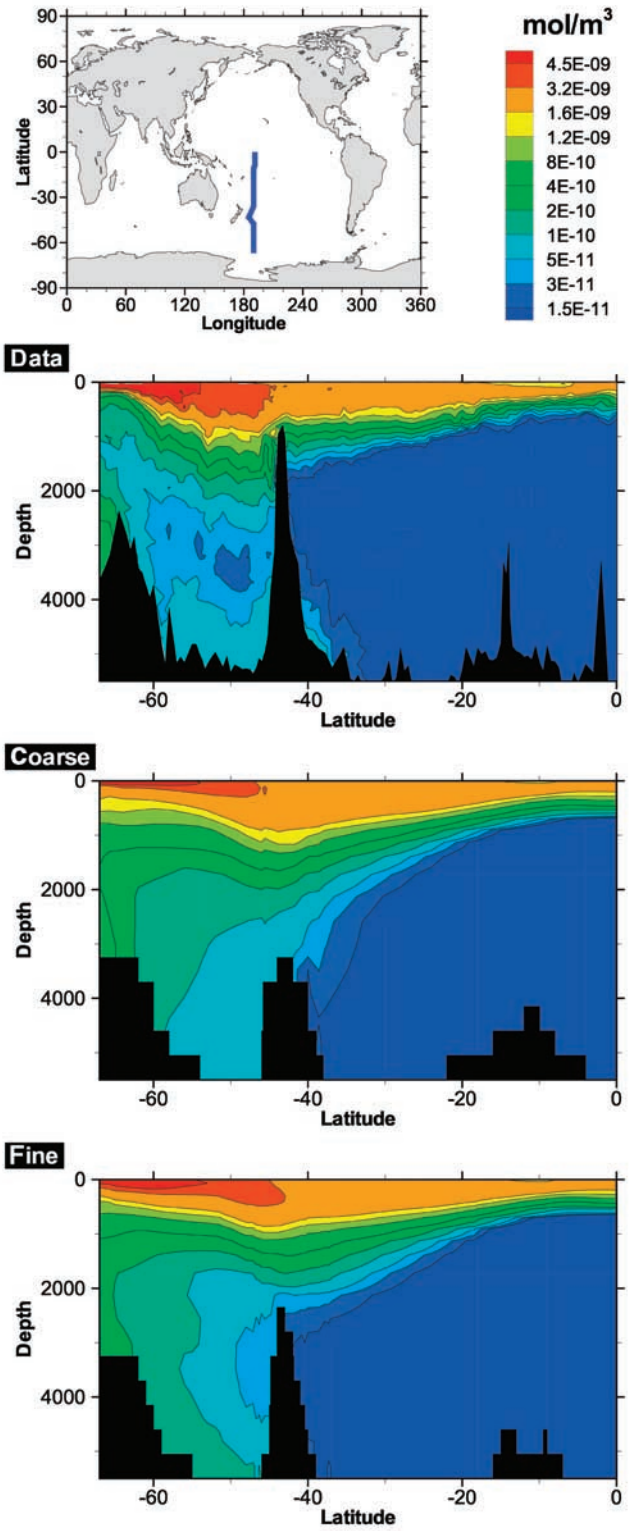

Figure 11. CFC-11 concentration along the P15S section [*WOCE Data Products Committee*, 2000]. Observations are from 1996; model results are from 1999.

but rather to pursue other approaches such as improved numerical methods, better parameterizations of sub-grid-scale processes, better forcing data, or perhaps local resolution increases.

[45] **Acknowledgments.** This work was funded by the Ocean Carbon Sequestration Research Program, Biological and Environmental Research (BER), U. S. Department of Energy. This work was performed under the auspices of the U. S. Department of Energy by University of California Lawrence Livermore National Laboratory under contract No. W-7405-Eng-48.

References

Boutin, J., and J. Etcheto, Long-term variability of the air-sea CO_2 exchange coefficient: Consequences for the CO_2 fluxes in the equatorial Pacific Ocean, *Global Biogeochem. Cycles*, *11*, 453–470, 1997.

Broecker, W. S., J. R. Ledwell, T. Takahashi, R. Weiss, L. Merlivat, L. Memery, T. H. Peng, B. Jahne, and K. O. Munnich, Isotopic versus micrometeorologic ocean CO_2 fluxes: A serious conflict, *J. Geophys. Res.*, *91*, 10,517–10,534, 1986.

Bryan, K., Accelerating the convergence to equilibrium of ocean climate models, *J. Phys. Oceanogr.*, *14*, 666–673, 1984.

Caldeira, K., and P. B. Duffy, Sensitivity of simulated CFC-11 distributions in a global ocean model to the treatment of salt rejected during sea-ice formation, *Geophys. Res. Lett.*, *25*, 1003–1006, 1998.

Caldeira, K., and P. B. Duffy, The role of the southern ocean in uptake and storage of anthropogenic carbon dioxide, *Science*, *287*, 620–622, 2000.

Danabasoglu, G., J. C. McWilliams, and W. G. Large, Approach to equilibrium in accelerated global oceanic models, *J. Clim.*, *9*, 1092–1110, 1996.

Doney, S. C., and J. L. Bullister, A chlorofluorocarbon section in the eastern North Atlantic, *Deep Sea Res., Part A*, *39*, 1857–1883, 1992.

Duffy, P. B., and K. Caldeira, Sensitivity of simulated salinity in a three-dimensional ocean model to upper ocean transport of salt from sea-ice formation, *Geophys. Res. Lett.*, *24*, 1323–1326, 1997.

Duffy, P. B., M. E. Wickett, and K. Caldeira, Effect of horizontal grid resolution on the near-equilibrium solution of a global ocean/sea-ice model, *J. Geophys. Res.*, *107*(7), 3075, doi:10.1029/2000JC000658, 2002.

Dutay, J.-C., et al., Evaluation of ocean model ventilation with CFC-11: Comparison of 13 global ocean models, *Ocean Model.*, *4*, 89–120, 2002.

England, M. H., Using chlorofluorocarbons to assess ocean climate models, *Geophys. Res. Lett.*, *22*, 3051–3054, 1995.

Esbensen, S. K., and Y. Kushnir, The heat budget of the global ocean: An atlas based on estimates from marine surface observations, *Tech. Rep., 29*, Clim. Res. Inst., Oreg. State Univ., Covallis, 1981.

Gent, P. R., and J. C. McWilliams, Isopycnal mixing in ocean general circulation models, *J. Phys. Oceanogr.*, *20*, 150–155, 1990.

Hellerman, S., and M. Rosenstein, Normal monthly wind stress over the world ocean with error estimates, *J. Phys. Oceanogr.*, *13*, 1093–1104, 1983.

Herzog, H. J., E. Adams, D. Auerback, and J. Caulfield, Technology assessment of CO_2 ocean disposal, *Rep. MIT-EL 95-001*, Energy Lab, Mass. Inst. of Technol., Cambridge, 1995.

Herzog, H. J., K. Caldeira, and E. Adams, Carbon sequestration via direct injection, in *Encyclopedia of Ocean Sciences*, vol. 1, edited by J. H. Steele, S. A. Thorpe, and K. K. Turekian, pp. 408–414, Academic, San Diego, Calif., 2001.

Killworth, P. D., D. Stainforth, D. J. Webb, and S. M. Paterson, The development of a free-surface Bryan-Cox-Semtner ocean model, *J. Phys. Oceanogr.*, *21*, 1333–1348, 1991.

Levitus, S., and T. Boyer, *World Ocean Atlas 1994*, vol. 4, *Temperature, NOAA Atlas NESDIS*, vol. 4, Natl. Oceanic and Atmos. Admin., Silver Spring, Md., 1994.

Magnesen, T., and T. Wohl, Biological impact of deep sea disposal of carbon dioxide, *Tech. Rep. 77A*, Nansen Environ. and Remote Sens., Cent., Bergen, Norway, 1993.

Marchetti, C., On geoengineering and the CO_2 problem, *Clim. Change*, *1*, 59–68, 1977.

McWilliams, J. C., Modeling the oceanic general circulation, in *Annual Review of Fluid Mechanics*, vol. 28, pp. 215–248, Annu. Rev., Palo Alto, Calif., 1996.

McWilliams, J. C., Oceanic general circulation models, in *Ocean Modeling and Parameterization*, edited by E. Chassignet, pp. 1–44, Kluwer Acad., Norwell, Mass., 1998.

Oberhuber, J. M., Simulation of the Atlantic circulation with a coupled sea ice-mixed layer-isopycnal general circulation model. part I: Model description, *J. Phys. Oceanogr.*, *23*, 830–845, 1993.

Orr, J. C., Estimates of anthropogenic carbon uptake from four 3-D global ocean models, *Global Biogeochem. Cycles*, *15*, 43–60, 2001.

Orr, J. C., et al., Ocean CO_2 sequestration efficiency from a 3-D ocean model comparison, in *Proceedings of the 5th International Conference on Greenhouse Gas Control Technologies*, edited by D. Williams et al., pp. 469–474, Commonw. Sci. and Ind. Res. Org., Collingwood, Aust., 2001.

Peng, T.-H., T. Takahashi, W. S. Broecker, and J. Olafsson, Seasonal variability of carbon dioxide, nutrients, and oxygen in the northern North Atlantic surface water: Observations and a model, *Tellus, Ser. B.*, *39*, 439–458, 1987.

Robitaille, D. Y., and A. J. Weaver, Validation of sub-grid scale mixing schemes using CFCs in a global ocean model, *Geophys. Res. Lett.*, *22*, 2917–2920, 1995.

Sarmiento, J. L., J. C. Orr, and U. Siegenthaler, A perturbation simulation of CO_2 uptake in an ocean general circulation model, *J. Geophys. Res.*, *97*, 3621–3645, 1992.

Takahashi, T., R. T. Williams, and D. L. Bos, *GEOSECS Pacific Expedition, Hydrographic Data*, vol. 3, Natl. Sci. Found., Washington, D. C., 1982.

Walker, S. J., R. F. Weiss, and P. K. Salameh, Reconstructed histories of the annual mean atmospheric mole fractions for halocarbons CFC-11, CFC-12, CFC-113, and carbon tetrachloride, *J. Geophys. Res.*, *105*, 14,285–14,296, 2000.

Walsh, J., A dataset on Northern Hemisphere sea ice extent, 1953–1976, *Rep. Glaciol. Data GD-2*, World Data Cent. for Glaciol., Boulder, Colo., 1978.

Wanninkhof, R., Relationship between wind speed and gas exchange over the ocean, *J. Geophys. Res.*, *97*, 7373–7382, 1992.

Warner, M. J., and R. F. Weiss, Solubilities of chlorofluorocarbons 11 and 12 in water and seawater, *Deep Sea Research, 32, Part*, 1485–1497, 1985.

Warner, M. J., and R. F. Weiss, Chlorofluoromethanes in South Atlantic Antarctic Intermediate Water, *Deep Sea Res.*, *39*, 2053–2075, 1992.

Weaver, A. J., and E. S. Sarachik, Reply: On the importance of vertical resolution in certain ocean general circulation models, *J. Phys. Oceanogr.*, *21*, 1702–1707, 1991.

Wickett, M. E., P. B. Duffy, and G. Rodrigue, A reduced grid for a parallel global ocean general circulation model, *Ocean Model.*, *2*, 85–107, 2000.

WOCE Data Products Committee, WOCE global data, version 2.0, *WOCE Rep. 171/00*, World Ocean Circ. Exp. Int. Program Off., Southampton, U. K., 2000.

Zheng, M., W. J. De Bruyn, and E. S. Saltzman, Measurements of the diffusion coefficients of CFC-11 and CFC-12 in pure water and sea water, *J. Geophys. Res.*, *103*, 1375–1379, 1998.

Zwally, H. J., J. Comiso, C. Parkinson, W. Campbell, F. Carsey, and P. Gloerson, *Antarctic Sea Ice, 1973–1976: Satellite Passive Microwave Observations*, Sci. and Tech. Inf. Branch, NASA, Washington, D. C., 1983.

K. Caldeira and P. B. Duffy, Climate and Carbon Cycle Modeling Group, Lawrence Livermore National Laboratory, 7000 East Ave., L-103, Livermore, CA 94550, USA. (kenc@llnl.gov; pduffy@llnl.gov)

M. E. Wickett, Center for Applied Scientific Computing, Livermore, CA 94550, USA. (wickett@llnl.gov)